

Ions Colliding with Cold Polycyclic Aromatic Hydrocarbon Clusters

A. I. S. Holm,¹ H. Zettergren,^{1,*} H. A. B. Johansson,¹ F. Seitz,¹ S. Rosén,¹ H. T. Schmidt,¹ A. Ławicki,² J. Rangama,² P. Rousseau,² M. Capron,² R. Maisonnay,² L. Adoui,² A. Méry,² B. Manil,³ B. A. Huber,² and H. Cederquist¹

¹*Department of Physics, Stockholm University, SE-106 91 Stockholm, Sweden*

²*Centre de Recherche sur les Ions, les Matériaux et la Photonique (CIMAP), CEA-CNRS-ENSICAEN, Bd Henri Becquerel, F-14070 Caen Cedex 05, France*

³*Laboratoire de Physique des Laser, CNRS, UMP 7538, Institut Galilée, Université Paris 13, 93430, Villetaneuse, France*

(Received 30 June 2010; published 19 November 2010)

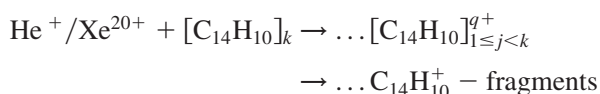
We report the first experimental study of ions interacting with clusters of polycyclic aromatic hydrocarbon (PAH) molecules. Collisions between 11.25 keV $^3\text{He}^+$ or 360 keV $^{129}\text{Xe}^{20+}$ and weakly bound clusters of one of the smallest PAH molecules, anthracene, show that $\text{C}_{14}\text{H}_{10}$ clusters have much higher tendencies to fragment in ion collisions than other weakly bound clusters. The ionization is dominated by peripheral collisions in which the clusters, very surprisingly, are more strongly heated by Xe^{20+} collisions than by He^+ collisions. The appearance size is $k = 15$ for $[\text{C}_{14}\text{H}_{10}]_k^{2+}$.

DOI: 10.1103/PhysRevLett.105.213401

PACS numbers: 36.40.Qv, 36.40.Wa, 95.30.Ft

Polycyclic aromatic hydrocarbon (PAH) molecules, their ions and their clusters are of high current interest in numerous scientific fields. PAH molecules and clusters may possibly be used for components in future nanoelectronic devices [1]. In environmental science, the burning of hydrocarbon based fuels and the wearing of car tires and roads provide some of the main PAH sources in air [2]. In this context, understanding reactions involving PAH molecules in the gas and condensed phases is crucial and has important implications for, e.g., health science [3]. In astrophysics the presence of neutral and charged PAH molecules and clusters is now considered to be firmly established through the observations of characteristic IR absorption features [4,5]. A number of studies of the photofragmentation of PAH molecules and clusters have been performed, but only one single study of the interaction between ions and PAHs has been reported this far and this was with a PAH monomer target [6]. However, interactions with keV ions in solar or stellar winds are as important as photon interactions in many astrophysical applications [7–10].

In the present study, which is the first on ions interacting with PAH clusters, the main aim is to investigate inherent PAH-cluster stabilities and the related fragmentation processes. In ion-cluster collisions charge and excitation energy may be induced locally in the clusters by peripheral collisions and fragment ion distributions may then reveal information on charge mobility and energy transport within the cluster. Here, we report on 11.25 keV $^3\text{He}^+$ and 360 keV $^{129}\text{Xe}^{20+}$ ions colliding with clusters of k anthracene molecules:



and compare with the fragmentation features when the same ions collide with isolated $\text{C}_{14}\text{H}_{10}$ monomers.

For He^+ we observe the expected strong decrease in the fragmentation of the individual $\text{C}_{14}\text{H}_{10}$ molecules upon clustering, but surprisingly, we do not see the corresponding decrease for Xe^{20+} where one would expect much less heating due to weak electronic and nuclear stopping processes at large electron transfer distances. In addition, we find that singly ionized clusters, $[\text{C}_{14}\text{H}_{10}]_k^+$, are too hot to stay intact on a microsecond time scale. In general $[\text{C}_{14}\text{H}_{10}]_k^{q+}$ clusters fragment by emitting neutral or singly charged $\text{C}_{14}\text{H}_{10}$ monomers or $[\text{C}_{14}\text{H}_{10}]_{j < k}^{q'+}$ clusters with $q' = 1$ for $1 \leq j < 15$ or with $q' = 1, 2$ for $j \geq 15$. The latter yields the $[\text{C}_{14}\text{H}_{10}]_k^{2+}$ appearance size $k = 15$.

Anthracene, $\text{C}_{14}\text{H}_{10}$, has three planar six-membered carbon rings in a row (c.f. Fig. 1). The lowest dissociation channels are H loss at 4.38 eV and C_2H_2 loss at 4.50 eV [11] and the first $\text{C}_{14}\text{H}_{10}$ ionization energy is 7.4 eV [12]. For neutral anthracene clusters the by far lowest dissociation energies correspond to losses of anthracene molecules or clusters. As an example the dissociation energy is only 0.35 eV [13] for $[\text{C}_{14}\text{H}_{10}]_2 \rightarrow 2\text{C}_{14}\text{H}_{10}$ dimer fragmentation. Calculations of PAH-cluster geometries are difficult due to the large areas of π - π interacting electrons, but indicate that the lowest energy structures for the smaller neutral clusters are 1D stacks while larger clusters form 3D structures [13–15].

The experiment was carried out at the ARIBE facility, Caen, France. The cluster target, $[\text{C}_{14}\text{H}_{10}]_k$, was obtained by evaporating anthracene powder at 120 °C inside a gas aggregation source with a flow of liquid nitrogen cooled helium gas to ensure that the $\text{C}_{14}\text{H}_{10}$ molecules are internally cold such that weakly bound $[\text{C}_{14}\text{H}_{10}]_k$ clusters form efficiently. This leaves far less than 1% monomers in the cluster target. The monomer $\text{C}_{14}\text{H}_{10}$ target was effused from a second oven operated at about 60 °C without cooling. The jets were crossed with the ion beams in the extraction region of a linear time-of-flight spectrometer

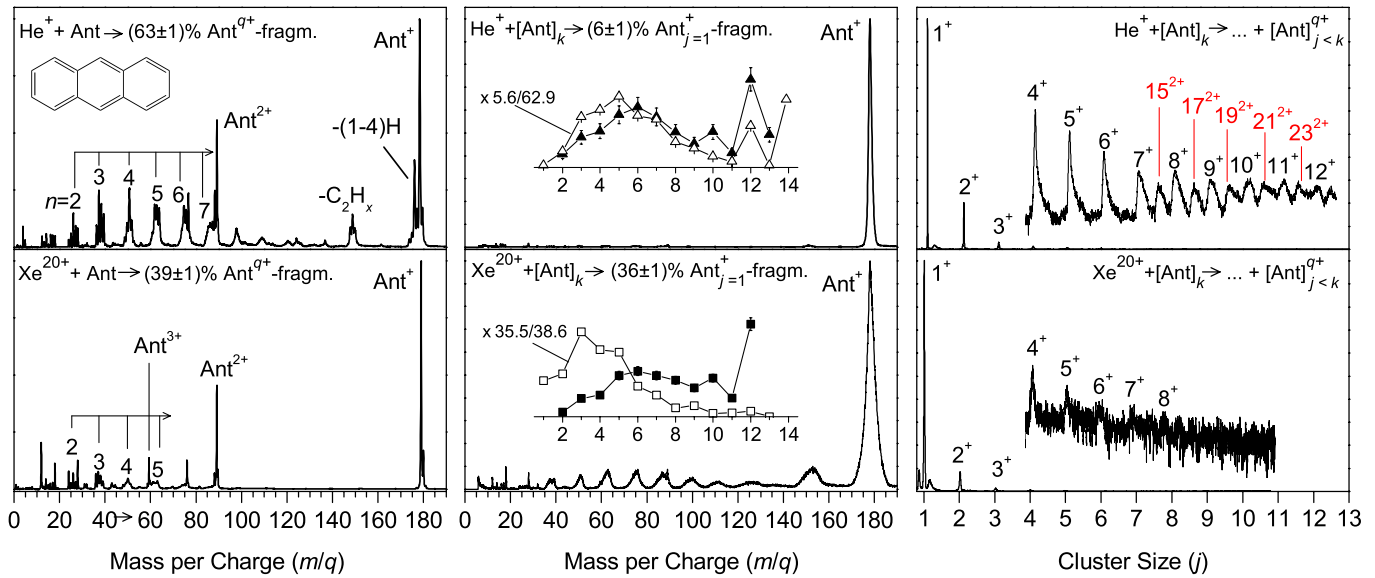


FIG. 1 (color online). Left panels: Mass-to-charge spectra for $\text{He}^+/\text{Xe}^{20+} + \text{C}_{14}\text{H}_{10}$ (monomer) collisions (molecular structure in the inset). Middle panels: Mass-to-charge spectra below 190 amu/e for $\text{He}^+/\text{Xe}^{20+} + [\text{C}_{14}\text{H}_{10}]_k$ (cluster) collisions. Insets show relative C_nH_x^+ intensity distributions as functions of n for the cluster (filled symbols) and monomer target (open symbols) scaled by the ratio between the cluster and monomer fragmentation efficiencies. Right panels: Size-to-charge spectra for fragment clusters, $[\text{C}_{14}\text{H}_{10}]_j^{q+}$, produced in $\text{He}^+/\text{Xe}^{20+} + [\text{C}_{14}\text{H}_{10}]_k$ collisions. Insets: zoom-ins for $j > 4$ with logarithmic intensity scales.

with which mass-to-charge spectra and kinetic energy release distributions were recorded [16]. The ion beams and the extraction voltages were pulsed with pulse lengths of $\sim 1 \mu\text{s}$ and with the extraction switched on $\sim 0.1 \mu\text{s}$ after passage of the ion pulse.

Mass spectra of anthracene *monomers* which are ionized and fragmented in collisions with He^+ or Xe^{20+} are shown in Fig. 1 (left panels). For He^+ , we observe singly and doubly charged intact $\text{C}_{14}\text{H}_{10}$ molecules (Ant^+ and Ant^{2+} in the figure), losses of H atoms, loss of C_2H_x from $\text{C}_{14}\text{H}_{10}^+$ and $\text{C}_{14}\text{H}_{10}^{2+}$, and smaller fragment ions, C_nH_x^+ , with $n = 1-11$. This type of bimodal distribution is similar to the ones observed for fullerene fragmentation where evaporation and multifragmentation processes compete [17,18]. For $\text{He}^+ + \text{C}_{14}\text{H}_{10}$ collisions the overall probability for fragmentation is $(63 \pm 1)\%$ and the C_nH_x^+ peaks with $n = 2-9$ are intense due to strong internal heating in small impact parameter collisions [6,19]. For Xe^{20+} , the overall fragmentation probability is $(39 \pm 1)\%$ and the relative intensity distribution changes in favor of C_nH_x^+ fragments with $n = 1-5$. Further, the H-loss and C_2H_x -loss channels become very weak and the peaks for $\text{Ant}^{2+/3+}$ and $\text{C}_{n<14}\text{H}_x^{2+}$ become stronger in relation to the $\text{C}_{n<14}\text{H}_{10}^+$ peaks. The differences between He^+ and Xe^{20+} collisions on monomers are readily explained. For He^+ the fragment spectrum is typical for thermally driven processes, while the Xe^{20+} fragment spectrum to a substantial extent is due to multiple electron removal at large distances [20] followed by Coulomb induced multifragmentation processes in which several small, charged fragments are emitted simultaneously [17,21].

The mass-to-charge spectra for He^+ or Xe^{20+} on anthracene *clusters* are shown in the middle and right panels of Fig. 1. The broad peaks in the rightmost panels are singly or doubly charged clusters stemming from fragmentation of still larger clusters. As expected the overall probability for forming fragments below the $\text{C}_{14}\text{H}_{10}$ mass in collisions with He^+ decreases strongly with the cluster target where the internal excitation energy is distributed within the cluster before fragmentation. Thus, $\text{C}_{14}\text{H}_{10}^+$ ions emitted as fragments from a cluster have less excitation energy than directly ionized molecules from the monomer target. The relative C_nH_x^+ intensity distributions, integrated over x and as functions of n (upper inset Fig. 1) are similar for He^+ on monomers (open symbols) and clusters (closed symbols). Thus, although the $\text{C}_{14}\text{H}_{10}^+$ fragmentation is much weaker in the cluster case, this similarity strongly suggests that fragments below 178 amu stem from thermally activated $\text{C}_{14}\text{H}_{10}^+$ also in this case. Doubly charged intact $\text{C}_{14}\text{H}_{10}$ ions are clearly observed with the monomer target but are absent with the $[\text{C}_{14}\text{H}_{10}]_k$ cluster target indicating that also charge is distributed on the clusters before fragmentation. The scenario that emerges for the $\text{He}^+ + [\text{C}_{14}\text{H}_{10}]_k$ collisions is thus that the He^+ projectile ionizes and excites the cluster in close, peripheral collisions. Charge and excitation energy distribute within the cluster before fragmentation which often yields singly charged monomers of which only a few, $(6 \pm 1)\%$, decay later.

The insets in the middle panels show that the relative C_nH_x^+ distribution for Xe^{20+} on clusters (closed symbols) is different from the one for Xe^{20+} on monomers (open symbols), but similar to both C_nH_x^+ distributions for He^+ .

Thus, the fragment distribution below 178 amu for $\text{Xe}^{20+} + [\text{C}_{14}\text{H}_{10}]_k$ is mainly due to thermally activated fragmentation of $\text{C}_{14}\text{H}_{10}^+$ ions emitted from the clusters as for $\text{He}^+ + [\text{C}_{14}\text{H}_{10}]_k$ collisions. Also, in the $\text{Xe}^{20+} + [\text{C}_{14}\text{H}_{10}]_k$ case charge must be distributed before $\text{C}_{14}\text{H}_{10}^+$ emission, as there are no doubly charged intact molecules or doubly charged C_nH_x fragments.

Zoom-ins on the $\text{C}_{14}\text{H}_{10}^+$ and $[\text{C}_{14}\text{H}_{10} - \text{C}_2\text{H}_x]^+$ regions are shown in Fig. 2. For He^+ on the monomer target we observe C_2H_2^- , C_2H_3^- , and C_2H_4 losses and there are strong contributions from pure H loss. The cluster target gives broad peaks for both projectiles reflecting the kinetic energy releases associated with the emissions of $\text{C}_{14}\text{H}_{10}^+$ from excited clusters. In the Xe^{20+} case, multiply charged clusters may be effectively produced and thus the fragment peaks are more strongly broadened than for He^+ due to the Coulomb repulsion in the fragmentation process. The C_2H_x loss peaks are rather symmetric and centered around $x = 2$ for the cluster targets, suggesting that these peaks mainly are due to C_2H_2 loss. We estimate typical internal excitation energies associated with C_2H_2 loss to be 7–8 eV for the four cases based on our measured intensities in the C_2H_2 -loss channels, calculated dissociation energies [11], and an Arrhenius expression with a preexponential factor of 4.7×10^8 , consistent with calculated C_2H_2 loss rates for naphthalene [22]. For He^+ on monomers the strong contributions from the $x = 3, 4$ loss channels and the long H-loss sequence suggest that the internal energy distribution extends to much higher energies, 4–5 eV per additional H loss in that case [11]. The similarity between the relative fragment intensity distributions for Xe^{20+} or He^+ on $\text{C}_{14}\text{H}_{10}$ clusters (c.f. insets in Fig. 1) is consistent with the similarity in estimated internal energies (7–8 eV). At first sight, however, it is then very surprising that $\text{Xe}^{20+} + [\text{C}_{14}\text{H}_{10}]_k$ collisions give much higher fragmentation yields for the emitted $\text{C}_{14}\text{H}_{10}^+$ monomers than the $\text{He}^+ + [\text{C}_{14}\text{H}_{10}]_k$ case. This must mean that a larger fraction of $\text{C}_{14}\text{H}_{10}^+$ emitted from clusters are excited with 7–8 eV in collisions with Xe^{20+} than in collisions with He^+ . There are two effects which may contribute to a larger yield of

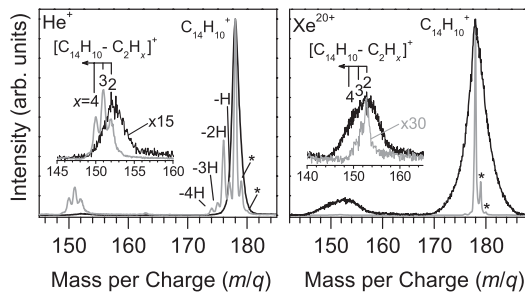


FIG. 2. Zoom-ins on the $\text{C}_{14}\text{H}_{10}^+$ - and C_2H_x -loss peaks for $\text{He}^+/\text{Xe}^{20+} + \text{C}_{14}\text{H}_{10}$ (grey curves) and $\text{He}^+/\text{Xe}^{20+} + [\text{C}_{14}\text{H}_{10}]_k$ (black curves) collisions. The insets are zoom-ins on the C_2H_x loss peaks. The asterisks mark the presence of carbon-13 isotopes.

sufficiently excited $\text{C}_{14}\text{H}_{10}^+$ monomers in the Xe^{20+} case: conversion of potential Coulomb energy into internal $\text{C}_{14}\text{H}_{10}^+$ excitation energy and capture of nonvalence electrons. In $\text{He}^{2+} + \text{C}_{60}$ collisions, removal of nonvalence electrons yields high internal excitation energies also for rather distant collisions with deposited energies of ~ 10 eV per removed electron [18]. Although such processes only occurred for smaller fractions of these ionizing collisions, the effect could be more important with projectile ions in higher charge states [23]. In addition, measurements of kinetic energy release distributions for highly charged fullerene dimers have shown that the potential Coulomb energy is to a substantial extent converted to internal excitation energy in the fragmentation process [24,25].

The $[\text{C}_{14}\text{H}_{10}]_j^{q+}$ -cluster peaks in the right panels of Fig. 1 are significantly broader than expected for processes in which electrons are removed without fragmentation of the cluster. Thus, we find that He^+ and Xe^{20+} collisions yield unstable clusters indicating that the energy transfer even for single electron removal is too high for small and intermediate clusters ($k < 13$) to remain intact on microsecond time scales. On one hand this seems reasonable considering the very small dissociation energies of neutral anthracene dimers (~ 0.35 eV), but on the other hand, nonfragmenting ionization is very important for, e.g., clusters of fullerenes [24–26] which have similar binding energies and even for argon dimers [27–29] which are much more weakly bound.

For He^+ , the $[\text{C}_{14}\text{H}_{10}]_{j < k}^+$ peak shapes change as a function of (final) cluster size, j , and a tail develops on the high-mass side (c.f. Fig. 1, right panels). As anthracene clusters have low binding energies and a first ionization energy similar to that of the monomer (7.4 eV), delayed fragmentation rather than delayed ionization is most likely the cause of these tails.

In Fig. 3, we show the relative intensity distributions of the singly charged cluster fragments $[\text{C}_{14}\text{H}_{10}]_{j < k}^+$ as functions of j . For both projectiles, the $\text{C}_{14}\text{H}_{10}^+$ fragment dominates with 70%–90% of the total fragment intensities. The intensity distribution in the Xe^{20+} case is typical for charge-driven multifragmentation processes and is very similar to those for fragmenting highly charged Na clusters

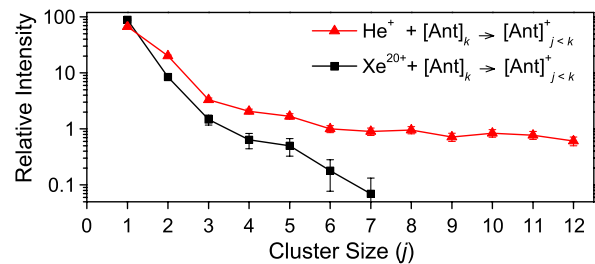


FIG. 3 (color online). Relative intensities of $[\text{C}_{14}\text{H}_{10}]_{j < k}^+$ clusters produced in Xe^{20+} (squares) and He^+ (triangles) collisions with clusters of k anthracene molecules $[\text{C}_{14}\text{H}_{10}]_k$.

[30]. Weakly bound clusters such as anthracene clusters, have similar ionization energies as their atomic or molecular building blocks. The dissociation energies for emissions of singly charged or neutral monomers should then be similar since the energies of the systems (cluster^{q+} + monomer) and (cluster^{(q-1)+} + monomer⁺) are similar. In such cases, the singly charged monomer may dominate among the charged fragments for multistep fragmentation processes. This behavior has been observed for singly charged aluminum and boron clusters [31–33] and we believe that this is also the main reason for the strong decrease in intensity with increasing fragment-cluster size, j , in Fig. 3. The steeper decrease with j for Xe²⁰⁺ is most likely due to the higher average cluster charge and the higher internal cluster excitation energy in that case.

In this Letter we have reported that keV ion collisions on small and intermediate size anthracene clusters ($k < 13$) always lead to prompt fragmentation following ionization and that the by far most likely fragments are singly charged anthracene monomers of which some later undergo unimolecular fragmentation. This behavior is different from weakly bound fullerene clusters for which ionization without fragmentation is dominant. Further we have shown that (i) clustering of anthracene molecules reduces the probability for molecular fragmentation strongly in single collisions with He⁺ as the excitation energy is distributed on the monomers in the cluster, (ii) charge is distributed on the whole cluster before fragmentation as only singly charged fragments are observed after collisions with Xe²⁰⁺, (iii) unexpectedly high internal excitation energies are induced in distant collisions with Xe²⁰⁺ leading to large probabilities for unimolecular fragmentation of internally heated C₁₄H₁₀⁺ most likely due to excitations in Coulomb explosions of multiply charge clusters and capture of non-valence electrons in the individual molecules, (iv) the appearance size for doubly charged anthracene clusters [C₁₄H₁₀]_k²⁺ is $k = 15$, and (v) the intensity decreases strongly with the numbers of intact anthracene molecules in the fragment clusters.

This very first experimental study of ions interacting with PAH clusters has thus revealed the main fragmentation pathways and an unusual instability of the present singly and multiply charged clusters produced in collisions with either He⁺ or Xe²⁰⁺. Here, we have used clusters of one of the smallest PAH molecules, anthracene, and one may ask if similar prompt fragmentation also occurs for clusters of larger PAH molecules or larger clusters than the ones considered here. Normally, clustering protects the individual molecules from fragmentation through the sharing of excitation energy (see, e.g., Ref. [34]), but here we find that the molecular damaging effect, very surprisingly, may be just as strong for clusters as monomers interacting with highly charged ions. While clusters of anthracene molecules are efficiently ionized in interactions with keV ions, small and

intermediate sized ($k < 13$) singly charged clusters cannot serve as nucleation sites for larger complexes in, e.g., astrophysical environments as they fragment promptly.

We acknowledge support from the Swedish Research Council, the ITS-LEIF Project (RII3 - 026015), and the Danish Council for Independent Research. We thank F. Noury and J.-M. Ramillon for technical support.

*Corresponding author: henning@fysik.su.se

- [1] A. J. Perez-Jimenez and J. C. S. Garcia, *J. Am. Chem. Soc.* **131**, 14 857 (2009).
- [2] C. P. Kaushik *et al.*, *Environmental Monitoring and Assessment* **122**, 27 (2006).
- [3] W. L. Xu and D. Warshawsky, *Toxicology and Applied Pharmacology* **206**, 73 (2005).
- [4] A. G. G. M. Tielens, *Annu. Rev. Astron. Astrophys.* **46**, 289 (2008).
- [5] E. Peeters *et al.*, *Astron. Astrophys.* **390**, 1089 (2002).
- [6] J. Postma *et al.*, *Astrophys. J.* **708**, 435 (2010).
- [7] L. Armus, *et al.*, *Astrophys. J.* **656**, 148 (2007).
- [8] E. R. Micelotta, A. P. Jones, and A. G. G. M. Tielens, *Astron. Astrophys.* **510**, A36 (2010).
- [9] E. R. Micelotta, A. P. Jones, and A. G. G. M. Tielens, *Astron. Astrophys.* **510**, A37 (2010).
- [10] M. S. Povich *et al.*, *Astrophys. J.* **660**, 346 (2007).
- [11] Y. Ling and C. Lifshitz, *J. Phys. Chem. A* **102**, 708 (1998).
- [12] D. Biermann and W. Schmidt, *J. Am. Chem. Soc.* **102**, 3163 (1980).
- [13] R. Podeszwa and K. Szalewicz, *Phys. Chem. Chem. Phys.* **10**, 2735 (2008).
- [14] M. Rapacioli, *et al.* *J. Phys. Chem. A* **109**, 2487 (2005).
- [15] M. Rapacioli and F. Spiegelman, *Eur. Phys. J. D* **52**, 55 (2009).
- [16] T. Bergen *et al.*, *Rev. Sci. Instrum.* **70**, 3244 (1999).
- [17] H. Cederquist *et al.*, *Phys. Rev. A* **61**, 022712 (2000).
- [18] A. Rentenier *et al.*, *Phys. Rev. Lett.* **100**, 183401 (2008).
- [19] T. Schlathölter *et al.*, *Int. J. Mass Spectrom.* **192**, 245 (1999).
- [20] A. Bárány *et al.*, *Nucl. Instrum. Methods Phys. Res., Sect. B* **9**, 397 (1985).
- [21] S. Tomita *et al.*, *Phys. Rev. A* **65**, 053201 (2002).
- [22] Y. A. Dyakov *et al.*, *Phys. Chem. Chem. Phys.* **8**, 1404 (2006).
- [23] A. Langereis *et al.*, *Phys. Rev. A* **63**, 062725 (2001).
- [24] H. Zettergren *et al.*, *J. Chem. Phys.* **126**, 224303 (2007).
- [25] H. Zettergren *et al.*, *Phys. Rev. A* **75**, 051201 (2007).
- [26] B. Manil *et al.*, *Phys. Rev. Lett.* **91**, 215504 (2003).
- [27] W. Tappe *et al.*, *Phys. Rev. Lett.* **88**, 143401 (2002).
- [28] T. Schlathölter and J. Postma (private communication).
- [29] U. Buck and H. Meyer, *Phys. Rev. Lett.* **52**, 109 (1984).
- [30] C. Guet *et al.*, *Z. Phys. D* **40**, 317 (1997).
- [31] L. Hanley and S. L. Anderson, *J. Chem. Phys.* **91**, 5161 (1987).
- [32] M. F. Jarrold, J. E. Bower, and J. S. Kraus, *J. Chem. Phys.* **86**, 3876 (1987).
- [33] O. Ingólfsson, H. Takeo, and S. Nonose, *J. Chem. Phys.* **110**, 4382 (1999).
- [34] B. Liu *et al.* *Phys. Rev. Lett.* **97**, 133401 (2006).